Optica Applicata, Vol. XXXIX, No. 1, 2009

A theoretical model of the human eye based on ultrasound and corneal data

MARTIN FALHAR[1*], JIŘÍ ŘEHÁK[2*]

[1]Faculty of Science, Palacky University, Olomouc, Czech Republic

[2]Department of Ophthalmology, University Hospital and School of Medicine, Palacky University, Olomouc, Czech Republic

[*]Corresponding authors: M. Falhar – M256@seznam.cz; J. Řehák – jiri.rehak@ocniklinikaol.cz

The purpose of this study was to create a theoretical model of the eye based on a comparison of the real spherical equivalent of the eye and the calculated value of the axial refraction. The main contribution of this model is that it enables calculation of the equatorial plane of the lens for accurate assessment of the IOL position for a spherical eye model. The Gullstrand model of the eye was used as the source eye model and this was modified for the purposes of this study. The axial refraction of the final model of the eye was compared with the spherical equivalent. The accuracy of the developed model was statistically confirmed using statistic tests. Individual calculation of the axial refraction using it shows that IOL calculation is possible without any general statistical presumptions. It permits the calculation of variables with an accuracy accepted by inferential statistics. The accuracy of this theoretical eye model however, is limited by extreme values of variables – an extreme value provides a less accurate result.

Keywords: biometry, theoretical eye model, lens, nucleus, intraocular lens (IOL), intraocular lens formula, axial refraction.

1. Introduction

To measure the intraocular lens (IOL) dioptric power, we need a theoretical model of the eye which allows us to make accurate calculations for each individual eye. A good model of the eye must be adaptable to statistical and biological variances. It is best if it does not contain statistical conclusions which could lead to inaccurate results in extreme cases. The goal here was to develop a model of the eye which maximally takes into account the individuality of each eye and which will not require any additional measuring variables. The variables are given by the standard procedures for IOL calculation.

The formulas need to incorporate the corneal parameters and axial positions of each optical surface. The corneal parameters were measured by autorefractokeratometer (ARK) which gives us the radius of curvature of the front corneal surface and a derived

keratometry parameter called K_{mean}. The axial positions of the optical surfaces were measured by ultrasonograph (USG). The depth of anterior chamber was measured with USG (ACD; this parameter also included the corneal thickness), the lens thickness L and the vitreum length V. The sum of ACD, L and V gave us the total axial length of the eye (AL).

The statistic describes the situation with a specific probability and no matter how probable the result is, the formula does not contain the theoretical principle of the optical imaging. Formulas for IOL power calculation work with these parameters and with statistical presumptions developed for the most probable value of the IOL power. All formulas give very good results for the normal axial length of the eye (22 mm to 24 mm). The formulas used produced a result with bigger variances for extreme axial length than the desirable value (high postoperative refraction).

Accurate calculation is vital for understanding what happens in imaging an object on the human retina. We can study this case if we reconstruct all eye parameters and calculate all important values. All formulas presume the situation after the lens extraction and the IOL calculation position mainly based on corneal and ACD parameters. The main problem is the correct calculation of the IOL position after the lens extraction. If we know all lens parameters we can precisely calculate the probable IOL position. Knowledge of the equatorial plane of the lens gives us very important information about the lens. The calculations based on the knowledge of the equatorial plane position allow us to calculate the IOL position strictly individually for each eye with respect to the main principles of imaging. This article completely describes the eye without additional parameters [1–3].

2. Methods

2.1. Measuring devices

The ultrasonograph data was measured on an OcuScan (Alcon Surgical) operating at 20 MHz. The anterior chamber depth ACD, lens thickness L and vitreum length V were measured with this device. These variables were acquired using a contact method with ultrasound velocity of wave in ACD of 1532 m/s, in L of 1641 m/s and in V of 1532 m/s. The sum of ACD, L and V gives us the axial length of the eye (AL).

The corneal parameters were measured on an autorefractokeratometer Canon RK-3. The main parameter was the radius of curvature of the front surface of the cornea (r_c) and the refraction of the eye was represented as the spherical equivalent SE. The r_c parameter was calculated as mean value of the radius in each main meridian. The r_c parameter recalculated to the dioptric power can be represented as K parameter. The spherical equivalent was assessed for vertex distance 12 mm. The SE parameter was recalculated as axial refraction of the eye (A'r).

2.2. Statistical characteristics of the samples

We used individual measurement due to large biological variances. The histograms and correlational trends of the basic biometric variables (N = 89 eyes, Pearson

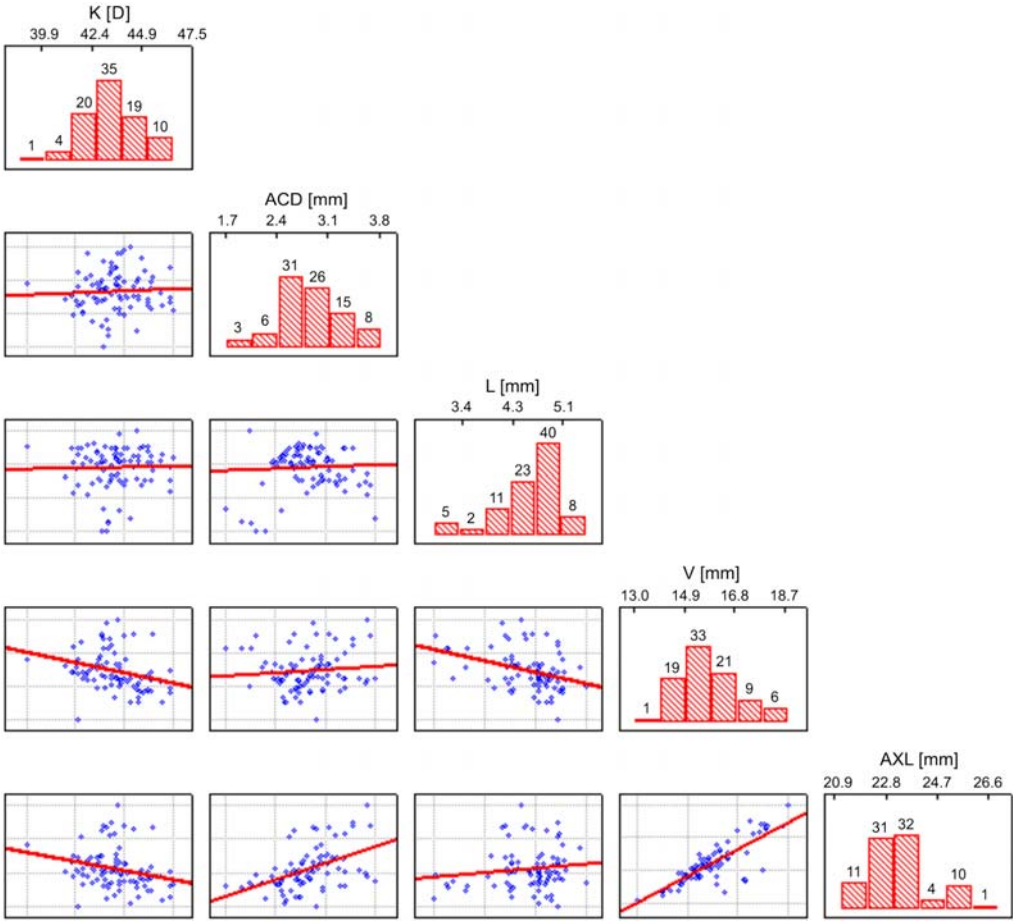

Fig. 1. Histograms and scatterplots of biometry eyes data; red lines show degree of the correlation (slope detect stronger dependence).

correlation coefficient r at P 0.05) level of significance are shown in Fig. 1 and Tab. 1. There was no significant correlation of anterior chamber depth, lens and axial length (important for IOL calculation). There was only a highly significant dependence (r = = 0.81) of vitreum length on axial length (which were of no use for IOL calculation)

T a b l e 1. Pearson correlation coefficients from the biometry data.

	K	ACD	*L*	*V*	AL
K	—	0.06	0.02	−0.30	−0.25
ACD	0.06	—	0.05	0.10	**0.49**
L	0.02	0.05	—	−0.37	0.13
V	−0.30	0.10	−0.37	—	**0.81**
AL	−0.25	**0.49**	0.13	**0.81**	—

and moderately significant correlation ($r = 0.49$) between anterior chamber depth and axial length (the coefficient was not strong enough for predictive purposes).

Six eyes suspected to have data with outlier values or data with large measuring errors were excluded during the creation of the eye model (more details are described in Section 4). The modified sample contained 89 eyes with an average age of 73.37 ± 9.36. The sample contained eyes with low or medium level cataract. The average spherical equivalent of the axial refraction was -0.75 D ± 3.39 D (minimum -10.77 D, maximum +9.31 D). The average absolute astigmatism established by means of corneal topography was 1.22 D $\pm$ 0.98 D (maximum 5.50 D). The average axial length was 23.28 mm $\pm$ 1.16 mm (minimum 21.13 mm, maximum 26.97 mm). The biometry characteristic histograms are shown in Fig. 2.

All data underwent statistic tests for normality. The biometry data characteristics are shown in Tab. 2.

2.3. Development and statistical methods

No physical model of the eye can be described using multivariate exploratory techniques, *e.g.*, factor analysis or principal component analysis. Factor analysis needs higher correlations between input variables ($r > 0.30$) and if we consider the low correlations (Tab. 1), the use of this test is not appropriate. Principal component analysis reduces the number of the variables. This can lead to the loss of fundamental relations between biometry data [4].

One reliable method for biometrical data evaluation is the exploratory regression analysis (ERA). The biometrical variables were processed by the results from ERA. The simulated calculation was made in a self-made program in Delphi (Borland) where the axial refraction was developed for this purpose. The entry biometric variables were treated by ERA and expressed relations were built into the calculation algorithm. The best-fit equation was calculated by the minimum residual square mean of the dioptric value between real axial refraction A'r and calculated axial refraction $A'r_{calc}$ [4].

The calculated $A'r_{calc}$ was matched with A'r using the Student *t*-test for dependent samples.

2.4. Theoretical model of the eye

The Gullstrand eye model (GEM) with parameters in the unaccommodated state was used as the source model. Table 3 shows basic starting values; Figure 3 shows the relationship of each variable.

Some variables were adopted as permanent, *e.g.*, index of refraction; other variables were modified according to the measured data.

2.4.1. Corneal parameters

The radius of curvature of the first corneal surface r_{C1} was derived from ARK. The parameter r_{C1} was calculated as the mean of the two radii in the main meridians. The radius of curvature of the second corneal surface r_{C2} was taken from the GEM

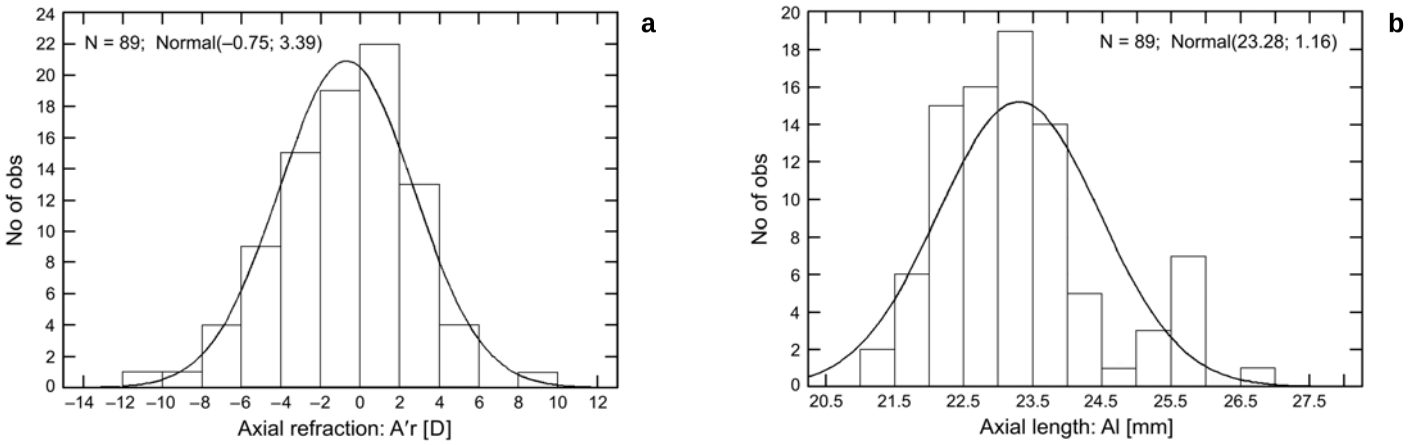

Fig. 2. The axial refraction histogram (**a**), the axial length histogram (**b**).

T a b l e 2. Biometry data characteristics (N = 89). This table shows the main statistics as mean, minimum, maximum, standard deviation) and basic statistical tests for normality: Kolmogorov–Smirnov test (K–S), Lilliefors test and Shapiro–Wilks test (S–W).

					K–S			S–W	
	Mean	Min.	Max.	Std. dev.	*d*	*p*	Lilliefors	*W*	*p*
A'r	–0.758	–10.775	9.31	3.398	0.07162	> 0.2	> 0.2	0.98905	0.66856
K	43.413	38.745	46.5	1.447	0.05974	> 0.2	> 0.2	0.98610	0.46404
ACD	2.909	1.724	3.886	0.429	0.05082	> 0.2	> 0.20	0.99019	0.75132
L	4.551	2.928	5.516	0.530	0.13252	<0.10	< 0.01	0.90331	0.00001
V	15.824	13.05	18.796	1.097	0.10219	> 0.2	< 0.05	0.96287	0.01204
AL	23.283	21.13	26.972	1.168	0.12105	< 0.15	< 0.01	0.93657	0.00030

T a b l e 3. Gullstrand eye model variables [7].

	Variable	Symbol	Value
Index of refraction	Cornea	n_C	1.376
	Aqueous humor, vitreum	n_{AH}, n_V	1.336
	Lens	n_L	1.386
	Lens nucleus	n_{LN}	1.406
Axial position [mm]	Corneal thickness	d_C	0.50
	Anterior chamber depth	d_{ACD}	3.10
	Lens thickness	d_L	3.60
	Lens nucleus thickness†	d_{LN}	2.42
	Lens nucleus distance†*	d_{LNshift}	0.55
	Vitreum length	d_V	16.80
	Axial length	AL	24.00
Radius of curvature [mm]	Front cornea surface	r_{C1}	7.70
	Back cornea surface	r_{C2}	6.80
	Front lens surface	r_{L1}	10.00
	Front lens nucleus surface	r_{LN1}	7.91
	Back lens nucleus surface	r_{LN2}	−5.76
	Back lens surface	r_{L2}	−6.00

†Calculated values of other variables from this table; * Distance from the first lens surface.

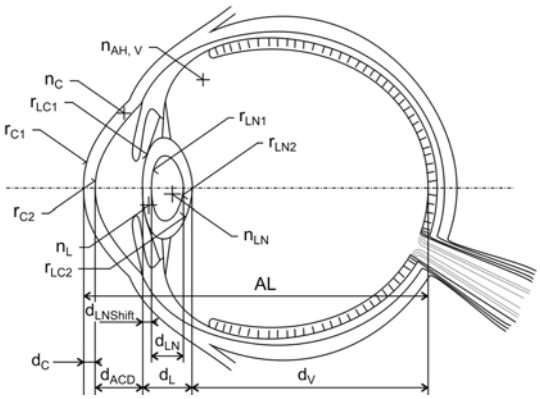

Fig. 3. Schematic eye model with variables.

(r_{C2} = 6.8 mm). Only advanced measurement procedures allow us to get the exact value of r_{C2} (for example Pentacam), but the small difference between the index of refraction of the cornea and the aqueous humor reduced the weight of this variable.

Correction was made for axial position on the corneal parameter r_{C1}. The sharp boundary between the retina and sclera detected by USG occurred at different distance than the sensory layer of the retina. For this reason we had to reduce the measured

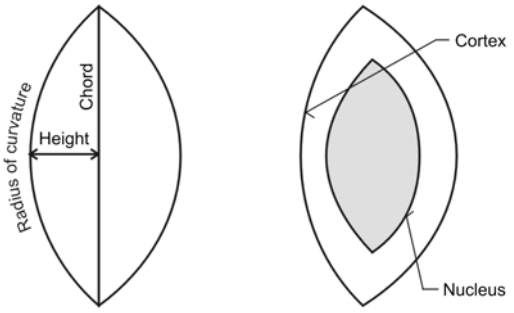

Fig. 4. Schematic lens model.

axial length by a specific value. Statistical analysis also requires a correction of r_{C1} gained from ARK where the origin value gives a result with a systematic hyperopic effect. It did not matter whether we did a correction individually for keratometry value and for axial length or if we combined both corrections into one.

The procedure for calculation of corneal parameters was as follows: The thickness of the cornea was taken from the GEM, so that $d_C = 0.5$ mm (this variable had no major influence on the final axial refraction). The ARK device gave us two corneal variables r_1 and r_2 in each main meridian:

$$r_{\text{mean}} = \frac{r_1 + r_2}{2} \tag{1}$$

$$r_{C1} = 0.4829\, r_{\text{mean}} + 3.999 \tag{2}$$

2.4.2. Lens parameters

Despite the fact that we calculated only in the paraxial spaces, the lens model is designed for peripheral areas, which allows us to evaluate the relations between the thickness of the lens, the equatorial position and the radii of the curvatures. This relation needs the condition of the connection between both lens surfaces at one point (equator). For this reason, mutual relations of the lens surfaces are conjugated by the equatorial position.

We can divide the lens into two parts: nucleus and cortex, where cortex contains nucleus. We can depict each of these parts as two segments of a circle with one common side (chord). The change of chord and radius of curvature for each optical surface affects the change of lens thickness. More details are shown in Fig. 4. The equation describing relation between chord C, height of the segment h and radius of curvature r is [5]:

$$C = 2\sqrt{h(2r - h)} \tag{3}$$

The degree and relations of each biometry variable were found by the exploratory regression analysis. We must hold the condition that the chord of the first part is equal

to the chord of the second part. Variables are described in Fig. 5. We can write the lens radius calculation:

$$r_{\mathrm{LC1}} = \frac{C_{\mathrm{LC}}^2 + 4h_{\mathrm{LC1}}^2}{8h_{\mathrm{LC1}}} \tag{4}$$

$$r_{\mathrm{LC2}} = \frac{C_{\mathrm{LC}}^2 + 4\,(L - h_{\mathrm{LC1}})^2}{8(L - h_{\mathrm{LC1}})} \tag{5}$$

$$r_{\mathrm{LN1}} = \frac{C_{\mathrm{LN}}^2 + 4h_{\mathrm{LN1}}^2}{8h_{\mathrm{LN1}}} \tag{6}$$

$$r_{\mathrm{LN2}} = \frac{C_{\mathrm{LN}}^2 + 4\,(L_{\mathrm{nucleus}} - h_{\mathrm{LN1}})^2}{8(L_{\mathrm{nucleus}} - h_{\mathrm{LN1}})} \tag{7}$$

We calculate the chord of the lens cortex C_{LC} from:

$$C_{\mathrm{LC}} = 0.9622\,L + 4.2 \tag{8}$$

The exploratory equation describing the chord of the lens nucleus C_{LN} shows greater statistical variance without the improving result. However, the whole lens nucleus is surrounded by lens masses with very similar refractive indices. For this reason, the constant value was taken from GEM for this case, in millimeters:

$$C_{\mathrm{LN}} = 7.62138 \tag{9}$$

The calculation of the segment height h_{LC1} is very important. The value of this variable provides information about the position of the equatorial plane. Analysis of this parameter gives:

$$h_{\mathrm{LC1}} = 0.81\,L \tag{10}$$

This simple result has two important aspects. Firstly, we note that the equatorial plane position and lens thickness are linearly dependent. Secondly, we can see the difference between h_{LC1} and h_{LC2}. In reality is $h_{\mathrm{LC1}} \approx h_{\mathrm{LC2}}$ and this relation is supported by the typical shape of the lens. However Eqs. (10), (4) and (5) give a different result: $h_{\mathrm{LC1}} > h_{\mathrm{LC2}}$. We can write this relation as $r_{\mathrm{LC1}} > r_{\mathrm{LC2}}$. This shows that the front lens surfaces must be steeper in our sample eyes. If we substitute the steeper aspherical surface with spherical surface, it will naturally increase

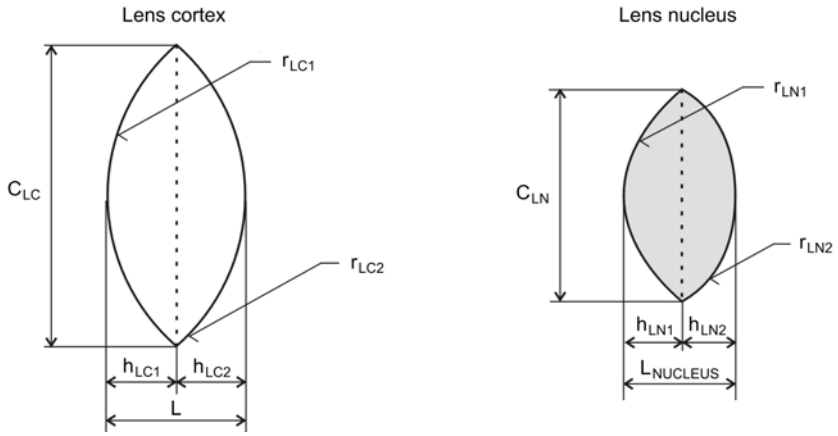

Fig. 5. Schematic lens model – notation.

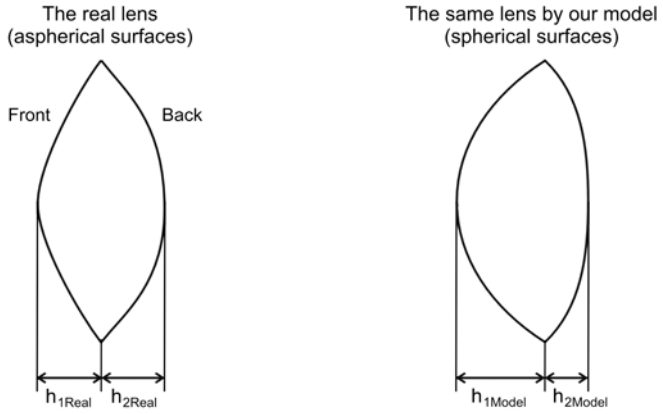

Fig. 6. The real lens can be described by an aspherical surface. The equatorial plane position in the real eye is mostly in the middle part of the lens ($h_{1Real} \approx h_{2Real}$). The majority of our eye data show the steeper aspherical surfaces of the real eye. If we substitute these aspherical surfaces for spherical surfaces we shift the equatorial plane further from the front surface ($h_{1Model} > h_{2Model}$).

the sagittal height of the spherical surface. This increase leads to an equatorial plane shift – more details in Fig. 6. This situation prevents us from making an easy prognosis of the probable equatorial plane position. Thus the model is useful only when working with a spherical radius of curvature. If we use an aspherical notation for radius of curvature, we cannot use this lens model [6].

The segment height for the lens nucleus shows a constant value (taken over from GEM; analyses do not give a significantly better result):

$$h_{LN1} = 0.6\, L_{nucleus} \tag{11}$$

The last important parameter is the nucleus shift from the first surface of the lens d_{LNShift} and lens nucleus thickness L_{nucleus}. Both parameters are derived from the L parameter:

$$d_{\mathrm{LNShift}} = 0.151\overline{6}\,L \tag{12}$$

$$L_{\mathrm{nucleus}} = 0.6719\overline{4}\,L \tag{13}$$

2.4.3. Axial refraction calculation

Axial refraction was calculated in the space of the first order (paraxial space). Dioptric powers of each optical unit were calculated by standard equations which were conjugated by Gullstrand equations for the dioptric power [7]:

$$\varphi_1 = \frac{n_2 - n_1}{r_1} \tag{14}$$

$$\varphi_2 = \frac{n_3 - n_2}{r_2} \tag{15}$$

$$\varphi_{12} = \varphi_1 + \varphi_2 - \frac{d}{n_2}\varphi_1\varphi_2 \tag{16}$$

The position of the principle planes was calculated for both optical surfaces [7]:

$$e = \frac{d}{n_2}\frac{\varphi_2}{\varphi_C}n_1 \tag{17}$$

$$e' = -\frac{d}{n_2}\frac{\varphi_1}{\varphi_C}n_3 \tag{18}$$

The details of the parameters are shown in Figs. 7 and 8. These are grouped as: corneal surfaces, front surfaces of the lens nucleus and cortex, back surfaces of the lens nucleus and cortex. Both lens pairs were conjugated into one lens complex. The lens complex was conjugated with corneal complex into a final unit (Fig. 6). From the position of the principle plane we can calculate the position of the focus which was calculated in terms of the physiological optic as axial refraction of the eye. The axial refraction was compared with spherical refraction from ARK (recalculated to the plane of the cornea) and was used in the statistical test for dependent samples.

3. Results

The correspondence between the calculated and the real axial refraction was the main criterion for evaluating the accuracy of the proposed eye model. The correspondence

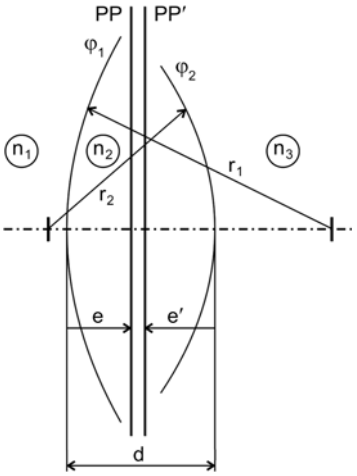

Fig. 7. Variable notation and their meaning.

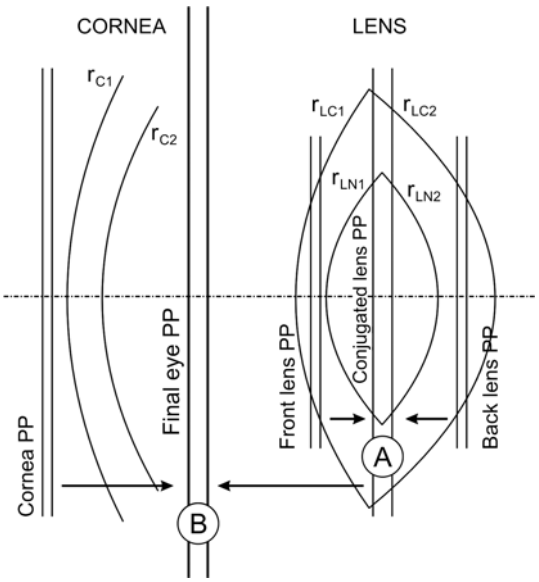

Fig. 8. Schematic model of the conjugation process of the principle planes (PP). First we calculate cornea, front lens and back lens PP. Therefore we conjugate front and back lens PP (situation A) and then complete we conjugate with cornea PP (situation B).

was tested by standard statistical procedures. Table 4 shows the result of the statistical test; Figure 9 shows the Box and Whiskers plot diagram.

The difference between A'r and $A'r_{calc}$ was evaluated too for accuracy evaluation of the reliability of the eye model. The difference (Fig. 10) we define as

$$\Delta A'r = A'r - A'r_{calc} \tag{19}$$

T a b l e 4. Statistical tests.

Student t-test for dependent samples								
	Mean	Std. dev.	*N*	Difference	Std. dev.	*t*	*df*	*p*
A'r	−0.758	3.398	89	−0.0205	2.27	−0.0854	88	0.932
$A'r_{calc}$	−0.737	2.776						
Pearson correlation coefficient 0.75								
Test for the variance correspondence								
Variance ratio					1.499			
Critical value					1.411			
Hypothesis for variances equality					Rejected*			$p = 0.027$
Robust test for the variance correspondence								
Variance ratio					1.499			
Critical value					1.875			
Test for the mean correspondence (equal variances)								
t-test					0.0442			
Critical value					1.974			
Hypothesis for the equality of means					$p = 0.965$			
Test for the mean correspondence (unequal variances)								
t-test					0.0442			
Critical value					1.974			
Hypothesis for the equality of means					$p = 0.965$			
Kolmogorov–Smirnov two sample test								
Difference DF					0.146			
Critical value					0.204			
Conclusion					Distributions are EQUAL			

*Possibilities lead to rejecting this hypothesis are discussed in Section 4.

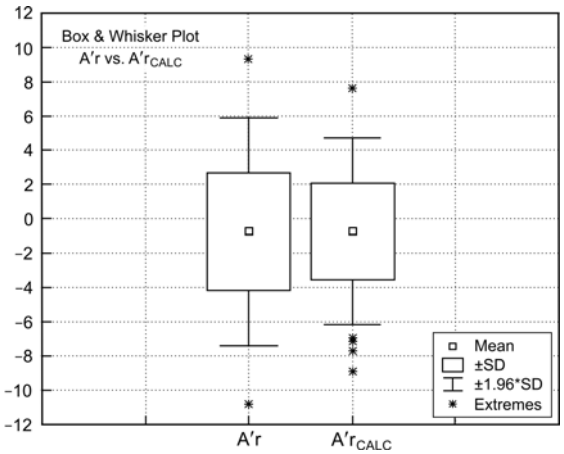

Fig. 9. Box and Whiskers plot diagram for real and calculated axial refraction.

4. Discussion and conclusions

The eye model developed here needs only four entry variables to compute the probable axial refraction and the relation between biometry variables. This eye description is reliable only in situations where we consider spherical surfaces. It is clear that the calculation based on four variables cannot describe the eye precisely. However this model provides results within the 95% confidence limits used in statistical tests and thus we can use it for superficial calculation of the axial refraction.

One of the final tests was rejected. Possible reasons for rejecting this hypothesis:

– The exploratory regression analysis leads to minimizing variances;

– The calculated axial refraction has more extreme points (Fig. 9);

– The evaluated data have a large measurement error (bias to mask the main principle of visualization);

– The developed eye model does not describe extreme cases accurately.

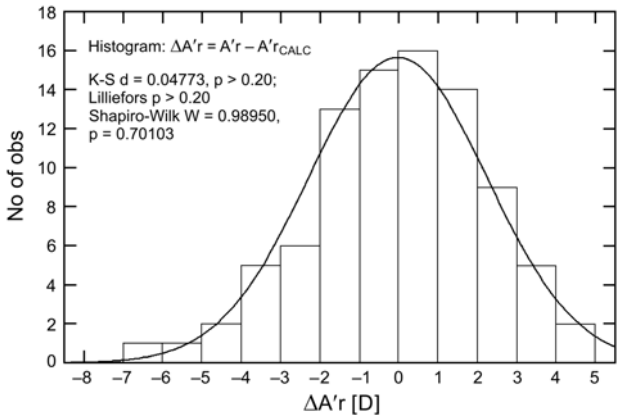

Fig. 10. Histogram of the differences between real and calculated axial refraction.

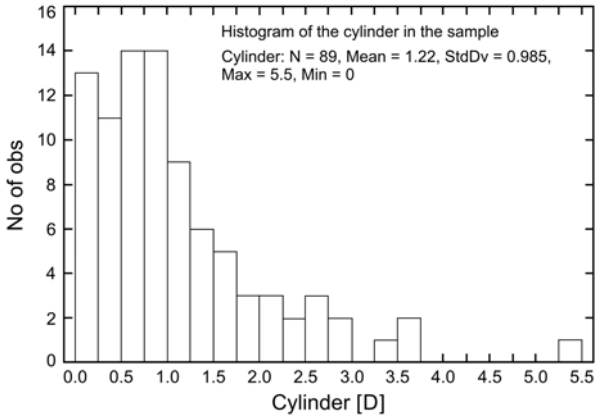

Fig. 11. The histogram of the cylinder in the sample.

We can explain the rejected statistical test using the mentioned reasons. The most probably is the extreme point value. There are two extreme points by real axial refraction and five extreme points by the calculated axial refraction. The value of extreme points has an influence on the variance of the statistical sample [4].

This model is developed on the SE description without correction of a number of cylinders. The cylinders can be responsible for an inaccurate result especially in cases with extreme values. The cylindrical distribution of the sample is shown in Fig. 11. It is possible to correct for the cylinder but we do not have enough information about the lens cylindricality. We cannot distinguish cases with a lens cylinder supported or inhibited by a corneal cylinder. This does not make likely the development of a reliable model of the eye with a cylinder factor.

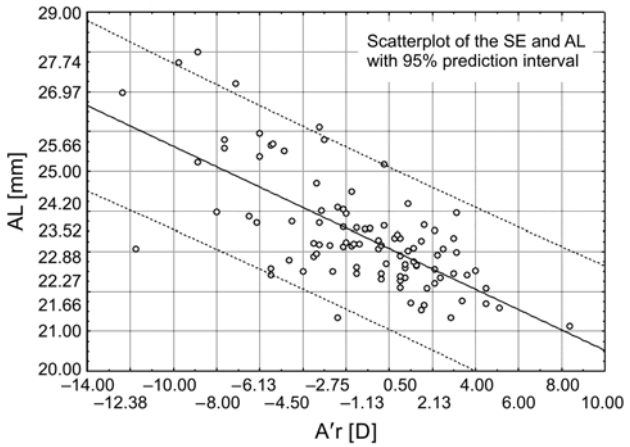

Fig. 12. The axial length and the axial refraction scatterplot show the outliers. Cases outside the prediction region were excluded.

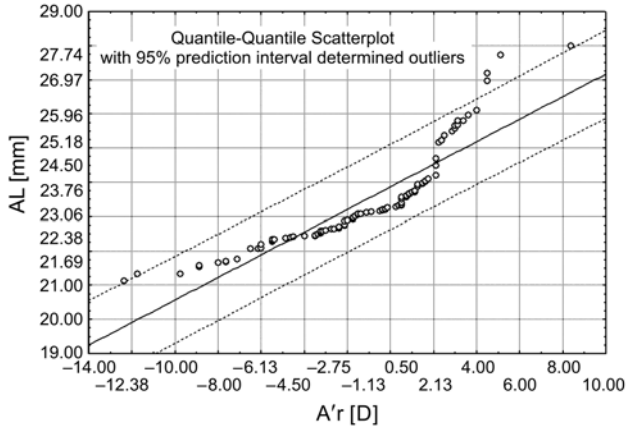

Fig. 13. The axial length and the axial refraction Q−Q graph determined outliers.

The original sample was 95 eyes. This sample was treated for useful data and for detection of possible detectable measurement errors. The scatterplot for AL and SE revealed six cases (Fig. 12). These cases were excluded from the sample. The quantile–quantile scatterplot was used as a confirming method with the same result (Fig. 13). These cases were classified as outliers and their use shows a big difference between the real and the calculated axial refraction (minimum −10.93, maximum +4.53). The excluded cases gave inconsistent results.

One way for improving the axial refraction calculation is by incorporating aspherical surfaces for a better description of the situation in the eye. The lens equatorial plane position calculation could be improved using an advanced lens model (better description of the relation between anterior and posterior radius).

This simple eye model can be advanced on any level of optical visualization field. The crystalline lens model can contain a shell structure [8], the nucleus lens model can be more detailed [6], the gradient-index lens can be used [9] or we can incorporate the lens refractive index which depends on age [10].

We can confirm that calculations can be done on these few variables. If we use a detailed eye model [11] we must recalculate equations due to aspherical surfaces but we can expect higher accuracy.

We can acquire the ultrasound data by contact, immersion or optical techniques. USG data for this model was acquired by contact measurements. The most accurate is the optical PCI method. Another is the immersion method. The contact method is the least accurate. This has the shortest measured axial length (and other parameters) because of the aplanation of the cornea during measurement. The mean error of the axial length acquired by optical and contact techniques is reported variously as 0.47 mm [12], 0.2 mm [13] and 0.04 [14]. The mean error of the anterior chamber depth is reported as 0.17 mm [15] or 0.32 [16]. A large variation is reported in different studies. We recommend the use of optical techniques but there remain conditions for using standard ultrasound techniques (*e.g.*, high density cataract).

Previous IOL formulas (SRK, SRK II, *etc*.) were built on statistical presumptions, *e.g.*, the anterior chamber depth was represented as a constant [2, 17]. Modern theoretical IOL calculation formulas are based on individual eye data. This premise was used in the presented eye model: we worked with each parameter for each eye individually. This assessment allows us to incorporate results of other authors. For example NAESER [18] IOL calculation formula works with an individual IOL design. Naeser method can be used for operating with variables applied in this model separately. The calculation of the IOL position is very important. The influence of the IOL shift is discussed by SIEDLECKI *et al*. [19]. The lens chord position calculated by our model reduces possible errors typical for a pure statistical IOL formula.

The limits of our model are caused by measurement accuracy. Extreme values lower the reliability. An axial length over 27 mm is typical for highly myopic eyes suffering from staphyloma which causes big error in measurement. The accuracy of the keratometer is reduced by extreme values. If we consider an eye with extreme axial

length and with an extremely steep cornea we can expect less accuracy of the proposed eye model.

Acknowledgments – I would like to express my gratitude to all those who gave me the possibility to complete this article. I want to thank my supervisor Dr. Řehák for giving me permission to use medical equipment and for letting me use departmental data.

References

[1] HOLLADAY J.T., *Standardizing constants for ultrasonic biometry, keratometry, and intraocular lens power calculations*, Journal of Cataract and Refractive Surgery **23**(9), 1997, pp. 1356–1370.

[2] HOLLADAY J.T., *Intraocular lens power calculations for the refractive surgeon*, Operative Techniques in Cataract and Refractive Surgery **1**(3), 1998, pp. 105–117.

[3] HILL W.E., *IOL power calculation accuracy: Advice on how to avoid common errors*, Cataract and Refractive Surgery Today, October 2003.

[4] MELOUN M., MILITKY J., *Kompendium statistického zpracování dat*, Academia, Praha 2002 (in Czech).

[5] BARTSCH H.J., *Matematické vzorce*, Academia, Praha 2006 (in Czech).

[6] HERMANS E., DUBBELMAN M., VAN DER HEIJDE R., HEETHAAR R., *The shape of the human lens nucleus with accommodation*, Journal of Vision **7**(10), 2007, p. 16/1.

[7] RUTRLE M., *Brýlová optika*, IDVPZ, Brno 1993 (in Czech).

[8] POPIOLEK MASAJADA A., *Numerical study of the influence of the shell structure of the crystalline lens on the refractive properties of the human eye*, Ophthalmic and Physiological Optics **19**(1), 1999, pp. 41–49.

[9] SIEDLECKI D., KASPRZAK H., PIERSCIONEK B.K., *Schematic eye with a gradient-index lens and aspheric surfaces*, Optics Letters **29**(11), 2004, pp. 1197–1199.

[10] GARNER L.F., OOI C.S., SMITH G., *Refractive index of the crystalline lens in young and aged eyes*, Clinical and Experimental Optometry **81**(4), 1998, pp. 145–150.

[11] POPIOLEK MASAJADA A., KASPRZAK H.T., *A new schematic eye model incorporating accommodation*, Optometry and Vision Science **76**(10), 1999, pp. 720–727.

[12] ELEFTHERIADIS H., *IOLMaster biometry: refractive results of 100 consecutive cases*, British Journal of Ophthalmology **87**(8), 2003, pp. 960–963.

[13] VERHULST E., VRIJGHEM J.C., *Accuracy of intraocular lens power calculations using the Zeiss IOL Master. A prospective study*, Bulletin de la Societe Belge d Ophtalmologie, No. 281, 2001, pp. 61–65.

[14] RAJAN M.S., KEILHORN I., BELL J.A., *Partial coherence laser interferometry vs conventional ultrasound biometry in intraocular lens power calculation*, Eye **16**(5), 2002, pp. 552–556.

[15] VETRUGNO M., CARDASCIA N., CARDIA L., *Anterior chamber depth measured by two methods in myopic and hyperopic phakic IOL implant*, British Journal of Ophthalmology **84**(10), 2000, pp. 1113–1116.

[16] KORANYI G., LYDAHL E., NORRBY S., TAUBE M., *Anterior chamber depth measurement: A-scan versus optical method*, Journal of Cataract and Refractive Surgery **28**(2), 2002, pp. 243–247.

[17] ELDER M.J., *Predicting the refractive outcome after cataract surgery: the comparison of different IOLs and SRK-II v SRK-T*, British Journal of Ophthalmology **86**(6), 2002, pp. 620–622.

[18] NAESER K., *Intraocular lens power formula based on vergence calculation and lens design*, Journal of Cataract and Refractive Surgery **23**(8), 1997, pp. 1200–1207.

[19] SIEDLECKI D., NOWAK J., ZAJAC M., *Placement of a crystalline lens and intraocular lens: retinal image quality*, Journal of Biomedical Optics **11**(5), 2006, p. 054012.

Received March 14, 2008
in revised form June 2, 2008